A Comparative Study on the CANDU-6 Reactivity Device Model Based on Wolsong-2 Physics Measurement Data

Chang Je Park[1] and Hangbok Choi[*1]
[1]*Korea Atomic Energy Research Institute*
Yuseong-gu, Deokjin-dong 150, Daejeon, Korea

Abstract

A benchmark calculation of a 713 MWe Canada deuterium uranium (CANDU) reactor was performed based on the physics measurement data of Wolsong-2 nuclear power plant by using WIMS-AECL, DRAGON, and RFSP codes. The benchmark calculation included sensitivity analyses on the number of energy groups, cross-section library, and the weighting spectrum of the homogenized lattice parameters. The effective multiplication factor, critical boron concentration, reactivity device worth and the flux distribution were estimated and compared with those obtained by the measurement and standard CANDU reactor physics design tools. In general, the prediction errors by WIMS-AECL, DRAGON and RFSP codes were within the acceptance limit for all the sensitivity calculations. The sensitivity calculations also showed that the calculation accuracy was improved when two energy groups were used especially for the prediction of the reactivity worth of strong absorbers such as mechanical control absorbers and shutoff rods. However, the prediction error increased when calculating the reactivity worth of the adjuster banks with two energy groups. Therefore a further study is recommended to obtain consistent results for the benchmark calculation.

KEYWORDS: CANDU, Reactivity Device, WIMS, DRAGON, Incremental Cross Section

1. Introduction

There are many computer codes typically used for a Canada deuterium uranium (CANDU) reactor physics analysis such as POWDERPUS-V [1] (PPV), WIMS-AECL [2], MULTICELL [3], SHETAN [4], DRAGON [5], and RFSP [6]. In addition, a Monte Carlo code MCNP [7] is also frequently used to supplement the diffusion- and transport-based reactor physics calculations. The standard physics design tool of the CANDU reactor is composed of PPV, MULTICELL and RFSP codes. The PPV is a lattice code especially developed for the natural uranium CANDU fuel based on empirical correlations. The MULTICELL is used to model the reactivity devices and structural materials in the CANDU reactor. The RFSP is a reactor analysis code designed for a reactor power calculation and a refueling simulation.

Advanced physics codes have also been developed and used for the design of new CANDU fuels such as the low-enriched uranium, mixed oxide fuel, thorium fuel and the DUPIC fuel [8-10]. At the same time, continuous effort is being made in the area of a benchmark test, including the cross-section library, a reactivity device modeling and the solution method, to reduce the design uncertainty of the CANDU fuel and reactor. Among the advanced physics

[*] Corresponding author, Tel. +82-42-868-2793, Fax +82-42-868-8580, Email: choih@kaeri.re.kr

codes, the WIMS-AECL is most widely used for the CANDU fuel lattice analysis owing to its capability of modeling a two-dimensional lattice and diverse isotopic data of the cross-section library. The WIMS-AECL provides homogenized cross-sections of the fuel lattice as well as the isotopic content of a fuel as a function of the fuel burnup. In order to model reactivity devices, the SHETAN was used to maintain the consistency within the solution method between the lattice and super-cell calculations [11]. Though the results of the benchmark calculation based on the WIMS-AECL and SHETAN are in general acceptable, it is true that the uncertainty level is a little higher than that obtained by the standard design and analysis tools.

There are several probable causes that result in a relatively large error when the reactivity devices are modeled by the SHETAN. For example, the working version of the SHETAN has a limitation in the number of energy groups and the incremental cross-sections are generated by a simple homogenization method. Of course, there could be other reasons that create an inconsistency between the measurement and simulation results. For example, the simulation results depend on the cross-section library. It is also possible that the weighting spectrum used to generate the homogenized cross-sections can create a difference in the simulation results. So far the natural uranium spectrum has been used for an incremental cross-section generation. However, there are also depleted uranium fuels in the fresh core, which is used for the benchmark calculation of the CANDU reactor.

In this paper, we have produced incremental cross-sections of the reactivity devices and structural material by the DRAGON code for the Phase-B condition of the Wolsong-2 nuclear power plant (NPP) [12]. For the purpose of an inter-comparison among the different solution models, the criticality was also calculated by the RFSP code based on the PPV and MULTICELL models. A brief description of the Phase-B condition used in this study is given in Sec. 2. The reactivity device model of the DRAGON is given in Sec. 3 for the incremental cross-section generation. The simulation results and the conclusion are given in Secs. 4 and 5, respectively.

2. Phase-B Condition for Wolsong-2 Reactor

The physics measurement data used for the benchmark calculation was obtained from the Phase-B test of the Wolsong-2 NPP performed in 1997. The Wolsong-2 NPP is a 713 MWe CANDU (CANDU-6) reactor and it is loaded with standard CANDU fuel bundles, which have 37 fuel rods. For the Phase-B condition (fresh fuel condition), the core is loaded with two different fuel types: 0.72 wt% natural uranium fuel and 0.52 wt% depleted uranium fuel. The depleted uranium fuels are scattered in the inner core region [13]. A CANDU-6 reactor has 380 fuel channels and each fuel channel contains 12 fuel bundles. There are four major reactivity devices to control the excess reactivity and adjust the power distribution: liquid zone controller (ZCU), adjuster (ADJ), mechanical control absorber (MCA), and shutoff rod (SOR), which are symmetrically placed on the vertical mid-plane of the core.

The Phase-B test is a part of the overall commissioning program of CANDU reactors and conducted to verify and analyze the physics design of the CANDU reactor. Most of the physics measurements are performed under a zero power operation condition. The critical operating conditions of the Phase-B measurements are as follows:

1) The average temperature of the coolant and moderator are 308.12 and 302.16 °K, respectively, for the initial core calculation.
2) The average ZCU water level is 16.94%.
3) The purity of the coolant and moderator are 99.63 and 99.84 wt%, respectively.
4) The MCA is inserted by 55%.

5) The critical boron concentration is 9.0 ± 0.5 ppm.

3. Reactivity Device Model

Incremental cross-section is a difference of the homogenized cross-sections of a 3-dimensional fuel lattice with and without a reactivity device. The incremental cross-sections of the reactivity device were calculated by the DRAGON code, which solves a 3-dimensional neutron transport equation including the condensation and homogenization of the lattice parameters to be used for the reactor calculations. The input cross-sections of a super-cell, composed of the fuel, tubes, coolant, moderator, and the reactivity device, are provided by the WIMS-AECL cross-section library. In the core calculation by the RFSP code, the existence of a given reactivity device is represented by adding incremental cross-sections to the homogenized cross-sections of a standard fuel lattice. Figure 1 shows the DRAGON models used to generate the incremental cross-sections, i.e., 3-dimensional lattices with and without a reactivity device.

Figure 1: DRAGON models for the reactivity device and fuel channel.

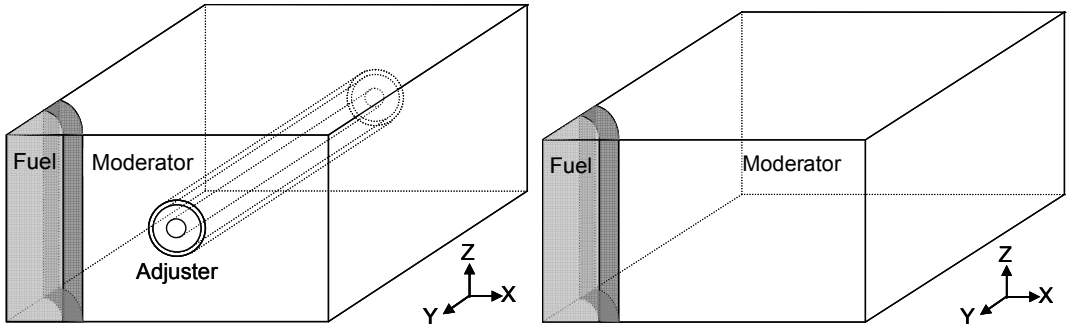

(a) Reactivity device (b) Fuel channel

Figure 2: DRAGON model for the structural material.

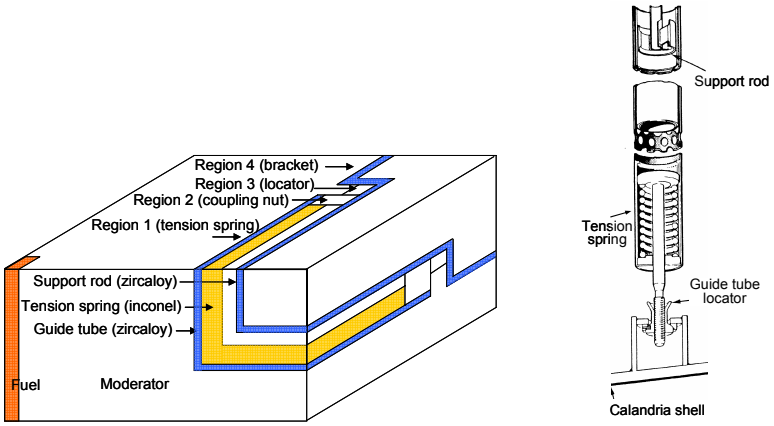

Structural materials such as the tension spring, locator, and the bracket are located near the calandria tank. For the structural materials located outside the fuel channel region, the incremental cross-sections are also generated by using a weak source material and a rectangular mesh structure by conserving the amount of structural material as shown in Fig. 2. The incremental cross-sections of these structural materials are generated by using the

difference of the homogenized cross-sections of the reflector material with and without the structural material. In the core calculation by the RFSP code, these structural materials are represented by adding incremental cross-sections to the reflector (heavy water) cross-sections.

Once the cell average cross-sections of a fuel lattice and the incremental cross-sections are prepared, the core calculations are carried out by the RFSP code to obtain the excess reactivity and power distributions. In the core calculation, the core is modeled by finite difference meshes for both the fuel and reflector regions. The number of meshes used for the core simulation is 44×36×22, which has been optimized through previous numerical tests [14].

4. Benchmark Calculation

The benchmark calculation was performed against the Phase-B physics measurement data of the Wolsong-2 NPP. The Phase-B test includes the first approach to a criticality and low power tests to verify the physics design and to evaluate the performance of the control and protective systems. In this study, the following cases were considered for the benchmark calculation:

- Approach to the first criticality,
- Calibration of the ZCU reactivity worth,
- Estimation of the reactivity device worth (ADJ, MCA, and SOR), and
- Thermal flux distribution.

During the Phase-B test, thermal flux scans were performed several times for various reactor configurations. The flux scans along a chord of the reactor core were made with a fission chamber. The flux distributions were calculated for the following cases:

Case 1) Nominal case
Case 2) MCA bank 1 inserted by 50% with all ADJs
Case 3) All MCAs inserted with all ADJs
Case 4) Without ADJ banks 1, 2, 3, and 4
Case 5) Without all ADJs.

In order to understand the probable cause of a prediction error, sensitivity calculations were also performed for a number of energy groups, the cross-section library and the weighting spectrum of the incremental cross-section. This sensitivity calculation for the incremental cross-section generation procedure can be categorized as follows:

Case a) 1.5 energy groups, ENDF/B-V library, and natural uranium spectrum
Case b) 1.5 energy groups, ENDF/B-VI library, and natural/depleted uranium spectrum
Case c) 2 energy groups, ENDF/B-VI library, and natural uranium spectrum
Case d) 2 energy groups, ENDF/B-VI library, and natural/depleted uranium spectrum.

5. Results and Discussion

Table 1 shows the effective multiplication factor and critical boron concentration based on the DRAGON model, which are compared with the results based on the MULTICELL and SHETAN models. It can be seen that the effective multiplication factors are predicted with a good accuracy for all the DRAGON cases. The critical boron concentrations are also within an acceptance limit of ±0.5 ppm.

The reactivity worth of the ZCU was obtained by directly changing the ZCU water level in the initial core. The simulation results of the average ZCU level worth are given in Table 2. Compared to the measurement results for the typical operating range of 20%~60%, the maximum difference between the measurement and calculation is 7.2% for the DRAGON

model with the ENDF/B-VI library. For an extended operating range of 20%~80%, the relative error is reduced to 4.9%, which is still within the acceptance limit of ±10 %.

Table 1: Effective multiplication factors and critical boron concentrations.

	MULTICELL	SHETAN (ENDF/B-V)	DRAGON (Case a)	DRAGON (Case b)	DRAGON (Case c)	DRAGON (Case d)
k_{eff}	0.99987	0.99648	0.99820	0.99653	0.99812	0.99796
Critical boron concentration	8.98 ppm	8.55 ppm	8.76 ppm	8.55 ppm	8.76 ppm	8.74 ppm

Table 2: Comparison of the ZCU level worth.

ZCU level	Measured	MULTI-CELL	SHETAN	DRAGON (Case a)	DRAGON (Case b)	DRAGON (Case c)	DRAGON (Case d)
20%□60%	0.07166 -	0.07266 (0.1%)	0.07368 (2.8%)	0.07494 (4.6%)	0.07682 (7.2%)	0.07251 (1.2%)	0.07166 (0.0%)
20%□80%	0.06769 -	0.06757 (-0.1%)	0.06938 (2.5%)	0.07089 (4.7%)	0.07097 (4.9%)	0.06841 (1.1%)	0.06614 (-2.3%)

The reactivity worth of the ADJ bank is given in Table 3. The maximum prediction error is 9% and 20% for the MULTICELL and SHETAN models, respectively. For the DRAGON model, the maximum error is between 12% and 18%, depending on the simulation cases. For all the cases, the total reactivity worth is under-predicted, which is probably due to an under-prediction of the thermal flux in the device region. The relative error of the total reactivity of the ADJ is less than 13% for the DRAGON model. Note that the allowable uncertainty of the total reactivity worth is ±15 % for the ADJ, MCA, and SOR.

Table 3: Reactivity worth of the ADJ bank.

ADJ bank	Measured reactivity (mk)	Relative error (%)					
		MULTI-CELL	SHETAN	DRAGON (Case a)	DRAGON (Case b)	DRAGON (Case c)	DRAGON (Case d)
1	1.36	5.0	-9.1	0.0	0.0	-7.5	-6.0
2	1.53	1.5	-8.6	0.2	-1.1	-8.2	-7.6
3	1.51	1.9	-8.2	0.6	1.2	-7.9	-6.6
4	2.33	-0.3	-13.3	-3.2	-2.8	-9.1	-8.3
5	1.77	-3.8	-15.3	-8.7	-9.3	-17.0	-16.4
6	1.79	-3.5	-14.9	-8.9	-8.4	-16.0	-15.4
7	3.37	-9.0	-19.8	-12.1	-11.3	-17.8	-16.6
Total	13.66	-2.3	-13.8	-5.8	-5.5	-12.8	-11.8

The relative error of the total reactivity worth is given in Table 4 for the MCA and SOR. For these strong absorbers, the prediction error is relatively large when compared to that of the ZCU and ADJ. For the MCA, the prediction error of the total reactivity worth is 7% and 8% for the MULTICELL and SHETAN models, respectively. The relative error of the total

reactivity worth of the MCA is distributed between 4% and 14%, when the DRAGON code is used. It can be seen that the reactivity worth is over-estimated for the strong absorber. For the SOR, the uncertainty level of the total reactivity worth prediction is similar to that of the MCA. Though the uncertainty level is within the acceptance limit for these devices, a further study will be necessary for the mesh structure of the core calculation model to obtain a better flux depression in the reactivity device region. The homogenization method of a 3-dimensional lattice also needs to be examined to see whether the individual reaction rate is preserved for the heterogeneous and homogeneous calculations or not.

Table 4: Total reactivity worth of the MCA and SOR.

	Measured reactivity (mk)	Relative error (%)					
		MULTI-CELL	SHETAN	DRAGON (Case a)	DRAGON (Case b)	DRAGON (Case c)	DRAGON (Case d)
MCA	7.7	7.4	8.0	14.9	13.9	6.6	6.0
SOR	45.4	6.4	10.5	13.6	12.5	5.2	4.0

The root-mean-square (RMS) error of the thermal flux prediction is summarized in Table 5. In this calculation, the average ZCU level was fixed at 40% and the boron concentration in the moderator was 8.7 ppm. The thermal flux at the detector position was obtained by interpolating the node-average flux of the RFSP calculation. When the ENDF/B-VI library was used (Cases c and d), the flux distribution was predicted well for all the cases within 12% Especially for the MCA insertion (Case 3), the RMS errors of Cases c and d were significantly reduced from 22% to 6% and from 14% to 9% for the horizontal and vertical flux distribution, respectively. The allowed uncertainty of the neutron flux estimation is 15% RMS.

Table 5: Prediction error of the thermal flux distribution.

		DRAGON (Case a)	DRAGON (Case b)	DRAGON (Case c)	DRAGON (Case d)
Case 1	Horizontal	12.7 %	12.3 %	11.9 %	11.9 %
	Vertical	10.0 %	8.1 %	5.9 %	5.9 %
Case 2	Horizontal	11.0 %	10.8 %	9.2 %	9.2 %
	Vertical	13.0 %	12.7 %	8.0 %	7.8 %
Case 3	Horizontal	21.5 %	21.6 %	6.1 %	6.1 %
	Vertical	14.3 %	12.8 %	9.4 %	9.4 %
Case 4	Horizontal	11.6 %	11.5 %	6.7 %	6.7 %
	Vertical	15.2 %	14.3 %	6.8 %	6.6 %
Case 5	Horizontal	13.2 %	13.5 %	6.5 %	6.5 %
	Vertical	15.9 %	15.2 %	7.1 %	7.1 %

For the case with natural and depleted uranium spectra (Case d), the RMS error of the thermal flux prediction was slightly lower when compared to the case with only a natural uranium spectrum (Case c) but the difference was very small. Here again, the effect of the number of energy groups on the flux calculation was dominant. The thermal flux distributions

are compared in Figs. 3 to 7 for the case with the 2-energy-group, ENDF/B-VI library and natural/depleted uranium spectrum (Case d), which is in principle the most realistic model.

Figure 3: Vertical and horizontal flux scan for Case 1.

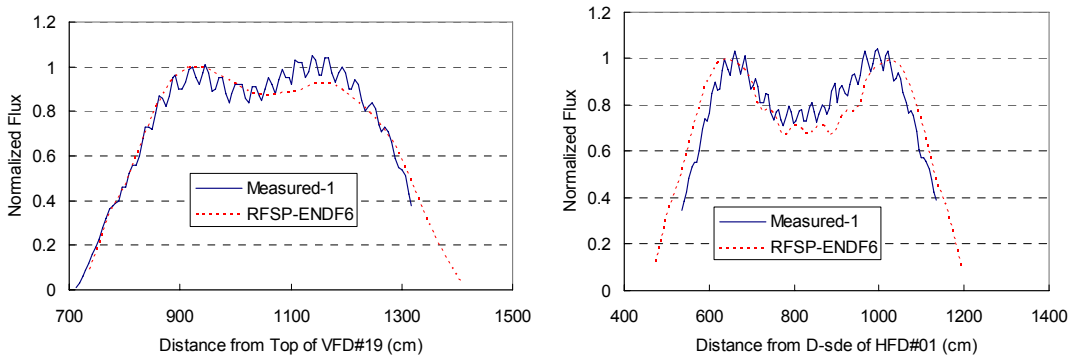

Figure 4: Vertical and horizontal flux scan for Case 2.

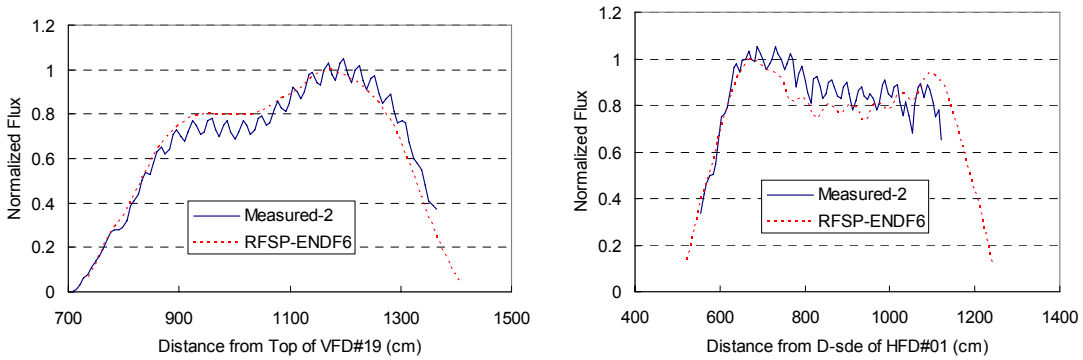

Figure 5: Vertical and horizontal flux scan for Case 3.

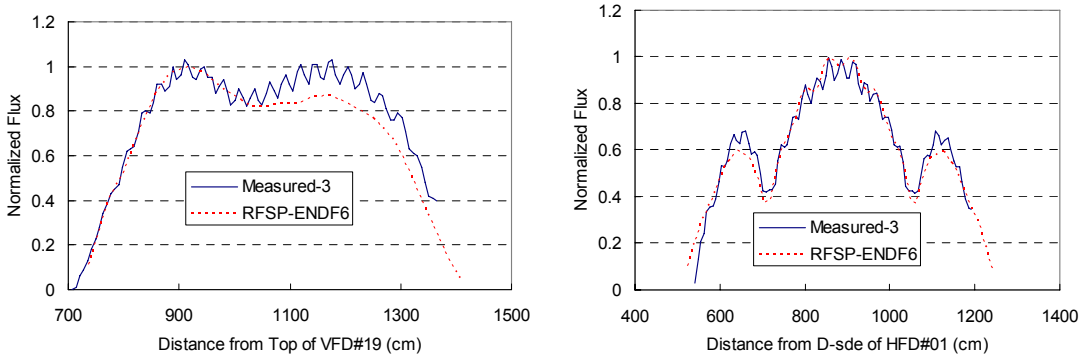

Figure 6: Vertical and horizontal flux scan for Case 4.

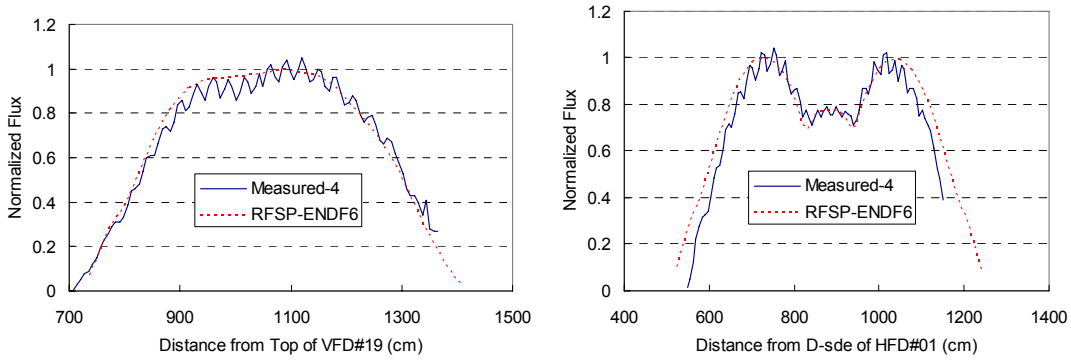

Figure 7: Vertical and horizontal flux scan for Case 5.

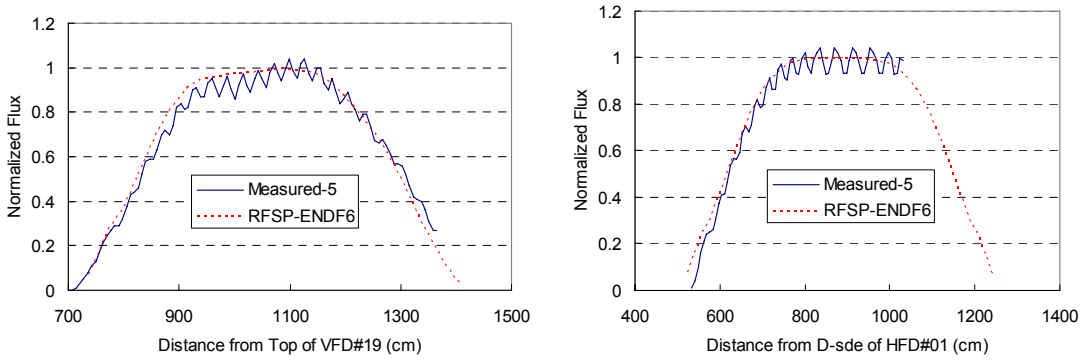

6. Summary and Conclusion

The reactivity devices and structural material of the CANDU-6 reactor were modeled by the DRAGON code to obtain the incremental cross-sections to be used for the core analysis. Then the benchmark calculations were performed with different numbers of energy groups, cross-section libraries and weighting spectra; and the results were compared with the physics measurement data of the Wolsong-2 NPP as well as the results obtained by the CANDU-6 reactor physics design tools. The results have shown that the DRAGON model predicts the criticality, reactivity device worth and the flux distribution with a reasonable accuracy. Though the prediction error of the total reactivity worth is within the allowable uncertainty limit for all the reactivity devices, the estimation of an individual rod worth still has a relatively large error. Therefore, it is recommended to further investigate the super-homogenization method of the incremental cross-section generation and the core mesh structure to improve the calculation results.

Acknowledgements

This work has been carried out under the nuclear research and development program of Korea Ministry of Science and Technology.

References

1) E.S.Y. Tin and P.C. Loken, "POWDERPUS-V Physics Manual," TDAI-31, Part 1, Atomic Energy of Canada Limited (1979).
2) J.V. Donnelly, "WIMS-CRNL: A User's Manual for the Chalk River Version of WIMS," AECL-8955, Atomic Energy of Canada Limited (1986).
3) A.R. Dastur et al., "MULTICELL User's Manual," TDAI-208, Atomic Energy of Canada Limited (1979).
4) H. Chow and M.H.M. Roshd, "SHETAN - A Three-Dimensional Integral Transport Code for Reactor Analysis," AECL-6787, Atomic Energy of Canada Limited (1980).
5) G. Marleau, A. Herbert and R. Roy, "A User Guide for DRAGON," IGE-174, Ecole Polytechnique de Montreal (1998).
6) D.A. Jenkins and B. Rouben, "Reactor Fuelling Simulation Program – RFSP: User's Manual for Microcomputer Version," TTR-321, Atomic Energy of Canada Limited (1993).
7) J.F. Briesmeister, ed., "MCNP – A General Monte Carlo N-Particle Transport Code, Version 4B," LA-12625-M, Los Alamos National Laboratory (1997).
8) D.F. Torgerson, P.G. Boczar and A.R. Dastur, "CANDU Fuel Cycle Flexibility," *Bulletin of the Canadian Nuclear Society*, **15**, 24 (1994).
9) P.G. Boczar, I.J. Hastings and A. Celli, "Recycling in CANDU of Uranium and/or Plutonium from Spent LWR Fuel," AECL-10018, Atomic Energy of Canada Limited (1989).
10) H. Choi, B.W. Rhee and H.S. Park, "Physics Study on Direct Use of Spent PWR Fuel in CANDU (DUPIC)", *Nucl. Sci. Eng.*, **126**, 80 (1997).
11) H. Choi, G. Roh, and D. Park, "Benchmarking MCNP and WIMS/RFSP Against Measurement Data – II: Wolsong Nuclear Power Plant 2," *Nucl. Sci. Eng.*, **150**, 37 (2005)
12) S.M. Kim, "Physics Post Simulation of Wolsong Nuclear Power Plant 2," Wolsong Nuclear Power Plant 1 (1997).
13) "Design Manual: CANDU 6 Generating station Physics Design Manual," 86-03310-DM-000, Rev.1, Atomic Energy of Canada Limited (1995).
14) D.A. Jenkins et al., "AMAD for Physics Simulations," Addendum to TDAI-440 Part I, Atomic Energy of Canada Limited, 1991.